Formulation and Evaluation of Metronidazole Loaded Chitosan Nanoparticles

Ruchika*, Himanshi

RPIIT Technical and Medical Campus, Karnal, India

www.ijsrm.humanjournals.com

ABSTRACT

The main objective of the present work was to prepare metronidazole (MTZ) loaded chitosan (CS) nanoparticles (NPs) intended for colon-specific delivery. The chitosan nanoparticles were prepared by the ionic gelation technique using sodium tripolyphosphate (TPP). Particle size distribution analysis confirmed the size ranges between 210-509 nm for chitosan nanoparticles and metronidazole loaded chitosan nanoparticles. Scanning Electron microscopy indicated smooth and spherical nanoparticles. FTIR and DSC showed no significant interactions between metronidazole and chitosan after encapsulation and cross-linking. Encapsulation efficiency of 69.3 % was achieved with a mass ratio of 0.5:1 (CS:MTZ). The nanoparticles exhibited bioadhesive properties, which diminished with increasing drug content. The results showed that the formulated nanoparticles have succeeded in controlling the release of metronidazole over 24 h period. Cumulative release data were fitted to an empirical equation to compare diffusional exponent (n), which indicated the Non-Fickian trend for drug release.

INTRODUCTION

The efficacy of many drugs is often limited by their potential to reach the site of therapeutic action. In most cases (conventional dosage forms), only a small amount of administered dose reaches the target site, while the majority of the drug distributes throughout the rest of the body in accordance with its physicochemical and biochemical properties. Therefore, developing a drug delivery system that optimizes the pharmaceutical action of a drug while reducing its toxic side effects *in-vivo* is a challenging task. One of the approaches is the use of colloidal drug carriers that can provide site-specific or targeted drug delivery combined with optimal drug release profiles. Among these carriers liposomes and nanoparticles have been the most extensively investigated.[1] Considerable research is being directed towards developing polymeric nanoparticles for drug delivery.[2] Polymeric nanoparticles which possess a better reproducibility and stability profiles. Nanoparticles have attracted a lot of attention of the pharmaceutical scientist in the drug delivery system due to versatility in targeting tissues, accessing deep molecular targets and controlling drug release.[3] Polymeric materials such as chitosan (CS) and poly-d,l-lactide-co-glycolide (PLGA) are used for synthesis of biodegradative nanoparticles. CS is a natural polysaccharide derived by partial deacetylation of chitin. Properties such as biodegradability, non-toxicity and good biocompatibility make it suitable for use in biomedical and pharmaceutical formulations.[4-8] During the last decade, there has been interest in developing site-specific formulations for targeting drug to the colon. Colonic drug delivery has gained increased importance, not just for the delivery of the drugs for the treatment of local diseases associated with the colon like Crohn's disease, ulcerative colitis, irritable bowel syndrome and constipation.[9-12] Chitosan is a promising polymer for colon drug delivery since it can be biodegraded by the colonic bacterial flora and it has mucoadhesive characteristic.[13] Nanoparticles based on CS receive currently increasing interest as they could control the rate of drug release, prolonging the duration of the therapeutic effect, and deliver the drug to specific sites in the body. CS can form nanoparticles using, amongst other methods, ionic gelation. The method is based on the gelation of CS when it comes in contact with specific polyanions due to the formation of inter- and intra-molecular cross-linkages mediated by the polyanions.[14-15] Metronidazole [2-(2-methyl-5-nitro- 1H- imidazol-1-yl) ethanol] is an amoebicide, antiprotozoal and antibiotic effective against anaerobic bacteria and certain parasites.[16] It is one of the most preferred drug of choice for intestinal amoebiasis, giardiasis, trichomoniasis, bacterial vaginosis,

Citation: Ruchika et al. Ijsrm.Human, 2016; Vol. 4 (4): 1-17.

2

surgical infections and duodenal ulcer associated with *Helicobacter pylori* infections, etc. The drug is to be delivered to the colon for their effective action against *E. histolytica* wherein the trophozoites reside in the lumen of the caecum and large intestine and adhere to the colonic mucus and epithelial layers. However, the pharmacokinetic profile of metronidazole indicates that the drug is completely and promptly absorbed after oral administration reaching a concentration in plasma of about 10 mg/mL approximately 1 h after a single 500 mg dose. The administration of this drug in conventional tablet dosage form provides minimal amount of metronidazole for local action in the colon, still resulting in the relief of amoebiasis however, associated with unwanted systemic effects.[17-20] Therefore, the objective of current investigation was to develop colon targeted metronidazole loaded nanoparticles. This is because colon targeted drug delivery system of metronidazole is associated with the following added advantages.

1. 98-100% bioavailability with 7-8 h half-life and hepatic metabolism of metronidazole
2. High physiochemical stability of metronidazole
3. Feasible analytical methodology (UV-spectrophotometer) for *in-vitro* studies of the developed delivery system[21]

2. MATERIALS AND METHODS

Pure Metronidazole was obtained by M/s Albert David Ltd. Ghaziabad, *ex gratis*. Chitosan was purchased from Yarrow Chem Products, Mumbai. Sodium tripolyphosphate was purchased from Titan Biotech Ltd. Bhiwadi, Rajasthan. All other materials and reagents used in this study were of analytical grade of purity.

2.1 Preparation of metronidazole loaded chitosan nanoparticles

Chitosan (CS) nanoparticles (NPs) were prepared based on ionic gelation between chitosan and sodium tripolyphosphate (TPP). CS solutions (0.2%, 0.3%, 0.4%, 0.5% and 0.6% w/v) were prepared by dissolving chitosan in glacial acetic acid (1% v/v) at an ambient temperature overnight. TPP solution (0.1% w/v) was prepared by dissolving sodium tripolyphosphate in distilled water. Subsequently, TPP solution was added dropwise to CS plus metronidazole solution stirring at 1000 rpm for 60 min. For the preparation of drug loaded nanoparticles, metronidazole (MTZ) was added to CS solution. Different drug concentrations *viz.* 0.15, 0.30, 0.45, 0.60 and 0.75 % w/v were used, keeping the chitosan concentration (0.3% w/v) and TPP

Citation: Ruchika et al. Ijsrm.Human, 2016; Vol. 4 (4): 1-17.

3

concentration (0.1% w/v) constant in each case. The pH of each formulation was adjusted with 1N NaOH and 0.1 N HCl at 4.5. Each formulation was centrifuged at 16000 rpm for 30 min. at 25°C and particles thus obtained were washed with 1% w/v mannitol solution. The supernatant thus obtained in each case were stored at 4°C until further use. The particles obtained after washing were transferred to labeled petri dishes and were finally lyophilized at approx. – 80°C for 48 h using lyophilizer. Table 1 depicts the concentration of CS, TPP and metronidazole used for development of different formulations.

Table 1: Composition of CS, TPP and metronidazole used in various formulation

Sr. No.	Formulation code	CS concentration in (mg)	TPP concentration in (mg)	Metronidazole concentration in (mg)
1	RM1	200	100	----
2	RM2	300	100	----
3	RM3	400	100	----
4	RM4	500	100	----
5	RM5	600	100	----
6	RM6	300	100	150
7	RM7	300	100	300
8	RM8	300	100	450
9	RM9	300	100	600
10	RM10	300	100	750

2.2 Characterization of metronidazole loaded chitosan nanoparticles

2.2.1 Particle size measurement

Average particle size of all the ten formulations (RM1 to RM10) of chitosan nanoparticles and metronidazole loaded chitosan nanoparticles were measured by Photon Correlation Spectroscopy (PCS) using ZS90 Zetasizer.

Citation: Ruchika et al. Ijsrm.Human, 2016; Vol. 4 (4): 1-17.

4

2.2.2 Determination of bioadhesive strength

The metronidazole loaded CS nanoparticles were immersed in a 50 mL glass beaker at $37^{o}C$ containing a phosphate buffer saline (pH 7.4) solution for 5 min in such a way that the solution just covered the nanoparticles. After nanoparticle wetting, a round fresh pig intestinal mucosa (PIM) with a diameter similar to that of glass beaker was placed on the surfaces so as to cover all the nanoparticles and remained for 5 min in contact with the nanoparticles. The intestinal mucosa with the attached nanoparticles was removed and the remaining nanoparticles on the glass beaker were dried at $60^{o}C$ till a constant weight was attained. The percentage of adhered nanoparticles (AN) was estimated using the equation 1.

$$AN\ (\%) = (W_{o} - W_{r}/\ W_{o})\ X\ 100$$

Where W_{o} is the initial weight of nanoparticles and W_{r} the remained unattached weight of nanoparticles.

2.2.3 Determination of drug Encapsulation Efficiency and Loading Capacity

Encapsulation Efficiency (EE) and Loading Capacity (LC) of all the formulations (RM6 to RM10) of metronidazole loaded chitosan nanoparticles were determined by measuring the ultraviolet absorption of the supernatant obtained in each case after centrifugation at 16000 rpm using UV-visible spectrophotometer at 319.5 nm. The percentage encapsulation efficiency and loading capacity of metronidazole loaded chitosan nanoparticles were calculated using eq. 2 and 3 respectively.

$$EE\ (\%) = \frac{W_{t} - W_{f}}{W_{t}}\ x\ 100 \qquad …(2)$$

$$LC\ (\%) = \frac{W_{t} - W_{f}}{W_{n}}\ x\ 100 \qquad …(3)$$

Where W_{t} represents the total amount of metronidazole; W_{f} is the amount of free metronidazole in the supernatant; and W_{n} is the weight of nanoparticles after freeze-drying. EE and LC of each formulation were determined in triplicate (n=3) and the mean EE and LC were finally reported.

Citation: Ruchika et al. Ijsrm.Human, 2016; Vol. 4 (4): 1-17.

5

2.2.4 *In-vitro* Dissolution studies

Drug release studies were carried out in a conical flask at 37°C and 75 horizontal strikes/min (horizontal shaker) where the suspension of metronidazole loaded chitosan nanoparticles (10 mg/50 mL) was placed. To compare the drug release under different pH conditions, the experiments were performed in 0.1 N HCl (pH 1.2), in phosphate buffer (pH 6.8) and in phosphate buffer saline (pH 7.4). Dissolution media and corresponding times included: 0.1 N HCl, pH 1.2 (120 min.), phosphate buffer pH 6.8 (120 min.), phosphate buffer saline pH 7.4 until complete release of the drug (24 h). At appropriate time intervals (30 min., 1, 2, 4, 8, 12, 16, 20, 24 h), 2 mL sample was withdrawn, replaced by 2 mL of fresh dissolution media, and samples were filtered through whatman filter paper 42. The samples were assayed spectrophotometrically at 278.5 nm, 319 nm and 320.5 nm for 0.1 N HCL, pH 6.8 phosphate buffer and pH 7.4 phosphate buffer saline respectively. The dissolution tests were performed under sink condition and in triplicate for each batch/formulation to calculate the mean values and standard deviations. One of the nanoparticle formulation would be selected for the determination of following parameters.

2.2.5 Morphological analysis

Scanning electron microscopy (SEM) was used in the morphological analysis of metronidazole loaded CS nanoparticles. The nanoparticles suspensions were spread on a glass plate and dried at room temperature. The dried nanoparticles were then coated with gold metal under vacuum and then examined.

2.2.6 Fourier Transform Infrared (FTIR) analysis

A small quantity of metronidazole loaded CS nanoparticles was mixed with 200 mg KBr and compressed to form tablets. These tablets were scanned, in transmission model, in the spectral region of 4000-400 cm^{-1}, using a resolution of 4 cm^{-1} and 32 co-added scans.

2.2.7 Differential Scanning Calorimetry (DSC) analysis

Differential Scanning Calorimetry (DSC) analysis of selected freeze dried metronidazole loaded CS NPs were carried out by Differential Scanning Calorimeter. 5 mg sample was placed onto a

Citation: Ruchika et al. Ijsrm.Human, 2016; Vol. 4 (4): 1-17.

6

standard aluminum pan, crimped and heated from 60 to 400°C at a constant rate of 10°C per min under continuous purging of nitrogen (20 mL/min). An empty sealed pan was used as reference. All samples were run in triplicate and the mean average values were calculated.

3. RESULTS AND DISCUSSION

3.1 Particle size measurement

Chitosan's ability of quick gelling on contact with polyanions relies on the formation of inter- and intramolecular cross linkages mediated by these polyanions. Nanoparticles are formed immediately upon mixing of TPP and chitosan solutions as molecular linkages were formed between TPP phosphates and chitosan amino groups. The ratio between CS and TPP is critical and controls the size and the size distribution of the nanoparticles. The size characteristics have been found to affect the biological performance of CS nanoparticles. For this reason, before the drug encapsulation into CS nanoparticles, the effect of CS/TPP ratio on the size characteristics of the nanoparticles was studied in order to find the optimum ratio that results to nanoparticles of low size and narrow size distribution. For this purpose, 5 different formulations (RM1 to RM5) were prepared by varying the concentration of CS from 0.2-0.6% w/v and keeping the concentration of TPP constant at 0.1% w/v. Table 2 depicts the particle size of chitosan nanoparticles obtained at varied concentrations of chitosan and Figure 1 shows the corresponding plots between CS/TPP mass ratio and particle size of nanoparticles (RM1 to RM5). From results, it can be said that there is a linear increase in particle size of nanoparticles with increase in CS/TPP mass ratio however, the increase was prominent at CS/TPP weight ratio of 6.0. Therefore, these linear relationships provide a simple processing window for manipulating and optimizing the nanosize for intended applications. In this study, chitosan/TPP with ratio 3:1 nanoparticles with sizes less than 350 nm was chosen for the preparation of drug loaded nanoparticles.

Five more different formulations of metronidazole loaded chitosan nanoparticles (RM6 to RM 10) were formed by varying the concentration of metronidazole 0.15, 0.30, 0.45, 0.60, 0.75 % w/v and keeping the chitosan concentration (0.3% w/v) and TPP concentration (0.1% w/v) constant. Table 3 depicts the particle size of metronidazole loaded chitosan nanoparticles at varied concentrations of metronidazole. The fig. 2 shows the corresponding plot. From the table

Citation: Ruchika et al. Ijsrm.Human, 2016; Vol. 4 (4): 1-17.

7

3 and fig. 2 it is evident that with the increase in MTZ/CS mass ratio, size of nanoparticles also increases.

Table 2: Particle size of chitosan nanoparticles at varied CS/TPP mass ratios

| Sr. No.	Formulation code	CS/TPP Conc. (w/v)	Particle size (nm)
1	RM1	0.2/0.1	317.7
2	RM2	0.3/0.1	327.7
3	RM3	0.4/0.1	330.9
4	RM4	0.5/0.1	351.4
5	RM5	0.6/0.1	480.9
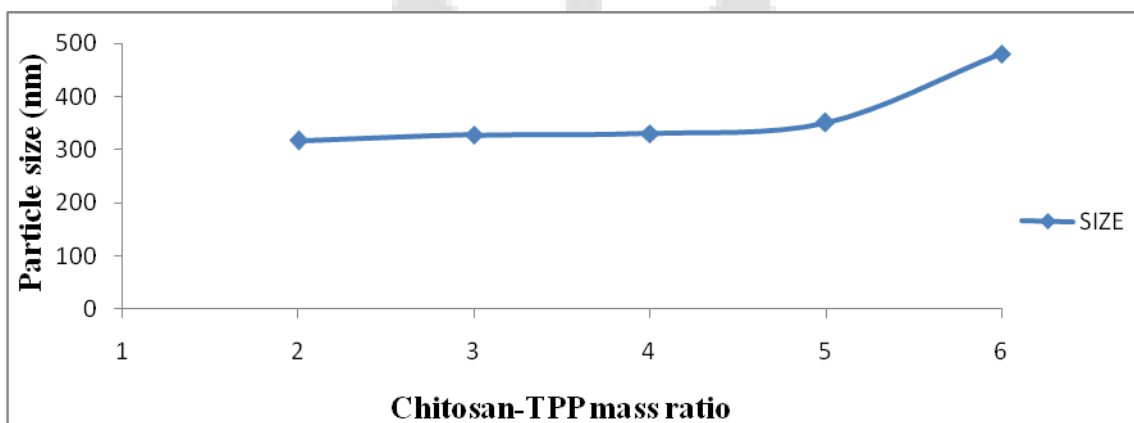
Figure 1: Effect of CS/TPP mass ratio on particle size of nanoparticles

Table 3: Particle size of metronidazole loaded chitosan nanoparticle

Sr. No.	Formulation code	MTZ/CS Conc. (w/v)	Particle size (nm)
1	RM6	0.15/0.3	210.4
2	RM7	0.30/0.3	309.7
3	RM8	0.45/0.3	343.9
4	RM9	0.60/0.3	451.7
5	RM10	0.75/0.3	509.4

Citation: Ruchika et al. Ijsrm.Human, 2016; Vol. 4 (4): 1-17.

8
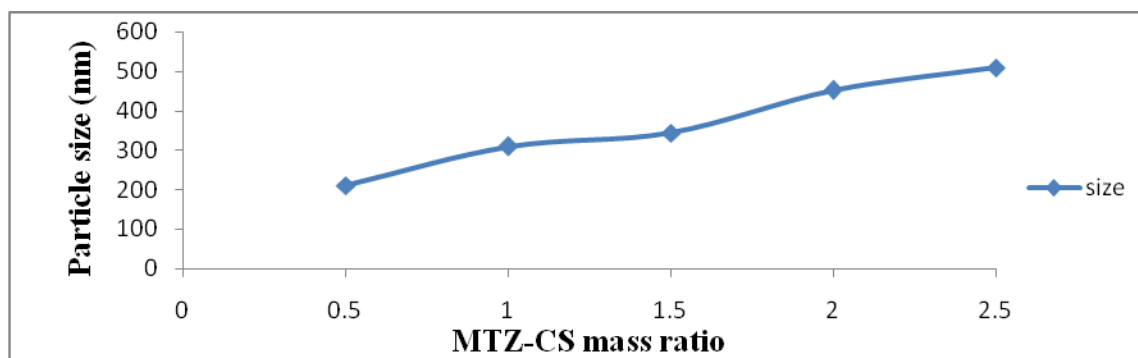
Figure 2: Effect of MTZ/CS mass ratio on particle size of nanoparticles

3.2 Determination of bioadhesive strength

In the current research work the mucoadhesive properties of metronidazole loaded chitosan nanoparticles were evaluated by measuring the weight fraction of nanoparticles which was adhered to PIM. In Table 4, the attached nanoparticles to PIM as weight (%) [AN%] are presented for chitosan nanoparticles prepared using different ratios of chitosan and TPP. An increase in nanoparticle size would decrease penetration in pig mucosa and the adsorption of mucin on nanoparticles surface (as the increase in size reduces the specific surface area of nanoparticles), leading to a decrease of the mucoadhesive strength of nanoparticles.

Also, as shown in Table 5, the drug content of the nanoparticles increases, the mucoadhesive strength of nanoparticles progressively decreases. As the drug amount in the nanoparticles increases, the amount of CS available for interacting with mucin or pig mucosa decreases, leading to lower mucoadhesive strength of nanoparticles.

Table 4: Adherence efficiency of different weight ratios between chitosan and TPP

Sr. No.	Formulation code	CS/TPP Conc. (w/v)	Adhered nanoparticles (AN) (%)
1	RM1	0.2/0.1	97±0.02
2	RM2	0.3/0.1	91±0.05
3	RM3	0.4/0.1	80±0.13
4	RM4	0.5/0.1	66±0.16
5	RM5	0.6/0.1	48±0.29

Citation: Ruchika et al. Ijsrm.Human, 2016; Vol. 4 (4): 1-17.

9

Table 5: Adherence efficiency of different weight ratios between chitosan and MTZ

Sr. No.	Formulation code	MTZ/CS Conc. (w/v)	Adhered nanoparticles (AN) (%)
1	RM6	0.15/0.3	91±0.09
2	RM7	0.30/0.3	82±0.11
3	RM8	0.45/0.3	68±0.14
4	RM9	0.60/0.3	56±0.26
5	RM10	0.75/0.3	30±0.32

3.3 Encapsulation Efficiency and Loading Capacity

Encapsulation Efficiency (EE) and Loading Capacity (LC) of metronidazole were calculated and the results were tabulated in Table 6. It is evident from results that increase of metronidazole concentration leads to a decrease of metronidazole encapsulation efficiency and an enhancement of loading capacity.

Table 6: Encapsulation Efficiency and Loading Capacity of metronidazole loaded Chitosan nanoparticles

Sr. No.	Formulation code	MTZ/CS conc. (w/v)	EE (%)	LC (%)
1	RM6	0.15/0.3	69.3±0.04	25.4±0.23
2	RM7	0.30/0.3	67.5±0.06	32.6±0.19
3	RM8	0.45/0.3	62.8±0.07	36.3±0.18
4	RM9	0.60/0.3	58.1±0.12	37.8±0.14
5	RM10	0.75/0.3	55.5±0.15	39.4±0.11

Citation: Ruchika et al. Ijsrm.Human, 2016; Vol. 4 (4): 1-17.

10

3.4 *In-vitro* Dissolution studies

Chitosan-based systems can be used for improving the retention and biodistribution properties of drugs applied topically at the released site. Table 7 and Figure 3 show *in-vitro* release profiles of metronidazole from chitosan nanoparticles in different dissolution media 0.1 N HCl (pH 1.2), in phosphate buffer (pH 6.8) and in phosphate buffer saline (pH 7.4). It shows an initial burst release of about 30–40% of metronidazole up to 1 hr, followed by a more gradual and sustained release phase for the following 24 h. The initial fast release might be the result of the rapid dissolution of the drug crystals located at or close to the surface of the nanoparticles or due to the rapid hydration of nanoparticles due to the hydrophilic nature of chitosan. After the burst release period, the rate of release fell as the dominant release mechanism was changed to drug diffusion through the chitosan matrix. The release medium penetrates into the particles and dissolves the entrapped drug and, therefore, it could be proposed that the major factor determining the drug release from nanoparticles is its solubilization or dissolution rate in the release medium. The release profiles of nanoparticles make it apparent that the entrapment of metronidazole in the nanoparticles can effectively sustain metronidazole release. Sustained drug release from the nanoparticles is important, as it would allow for a prolonged residence of the drug at the surface of the release site, increasing drug bioavailability and prolonging the therapeutic effect. Also, the release profiles of different metronidazole concentrations from CS nanoparticles in dissolution media in at 37±0.5°C are shown in Figure 3. The release profile of nanoparticles with different metronidazole concentrations showed that the overall ''rate'' of drug release (i.e. the fraction of drug content of the nanoparticles released at a given time) tended to become higher as the drug proportion in the nanoparticles increased. The differences in the release of the drugs due to differences in concentrations of drug within the particles led to differences in the mechanism of diffusion. It is likely that differences in the concentrations within the particles will lead to differences in the partitioning of the drugs between the solution state within the particles, as well as having a direct influence on the overall flux through the coats.

Data obtained from the *in-vitro* release studies were fitted to various kinetic equations such as zero-order, first-order, Higuchi model and Korsmeyer-Peppas model. The results are shown in Table 8. The optimum model was selected based on the correlation coefficient value (r^2) of

Citation: Ruchika et al. Ijsrm.Human, 2016; Vol. 4 (4): 1-17.

11

various model, and the results indicated that the drugs release from nanoparticles fitted Higuchi model best from the above four models.

The Korsmeyer–Peppas equation was also used to determine the mechanism of drug release. The initial portion of cumulative drug release (%) Vs. time can be expressed by followed equation

$$\frac{M_t}{M_\infty} = Kt^n$$

where Mt/M∞ is the fraction of drug released at time t, k is the kinetic constant and n is the diffusion exponent; the n value was calculated and presented in Table 8. For the formulation with the feed ratio 0.5:1.0, the n value of the MTZ was 0.588 suggesting that the drug was released by Anomalous transport mechanism (non- fickian diffusion).

Table 7: Dissolution data of formulations

Time	Cumulative % Release ± SD (n=3)				
(h)	RM6	RM7	RM8	RM9	RM10
0	0	0	0	0	0
0.5	23.667±1.49	25.272±1.46	26.444±0.83	31.569±1.40	36.458±1.58
1	32.403±2.31	36.208±1.35	38.028±1.54	40.500±2.81	45.333±1.43
2	45.472±1.83	45.210±1.75	48.972±1.17	50.652±1.57	52.153±1.29
4	55.931±1.67	56.625±1.18	57.222±1.16	65.694±1.43	69.232±1.16
6	60.153±0.93	62.069±1.52	65.694±1.43	68.431±2.24	73.467±0.88
8	65.222±1.52	67.249±1.91	67.431±0.88	72.139±1.32	76.764±2.05
12	68.667±1.46	71.278±1.47	72.139±1.32	73.944±2.34	78.625±1.90
16	71.375±1.29	72.431±1.80	74.333±1.71	78.056±1.63	81.931±1.52
20	74.286±1.60	77.206±1.72	81.472±1.29	82.597±0.26	84.819±1.21
24	79.667±1.07	80.724±1.39	82.597±0.26	85.625±1.54	87.000±1.77

Citation: Ruchika et al. Ijsrm.Human, 2016; Vol. 4 (4): 1-17.

12

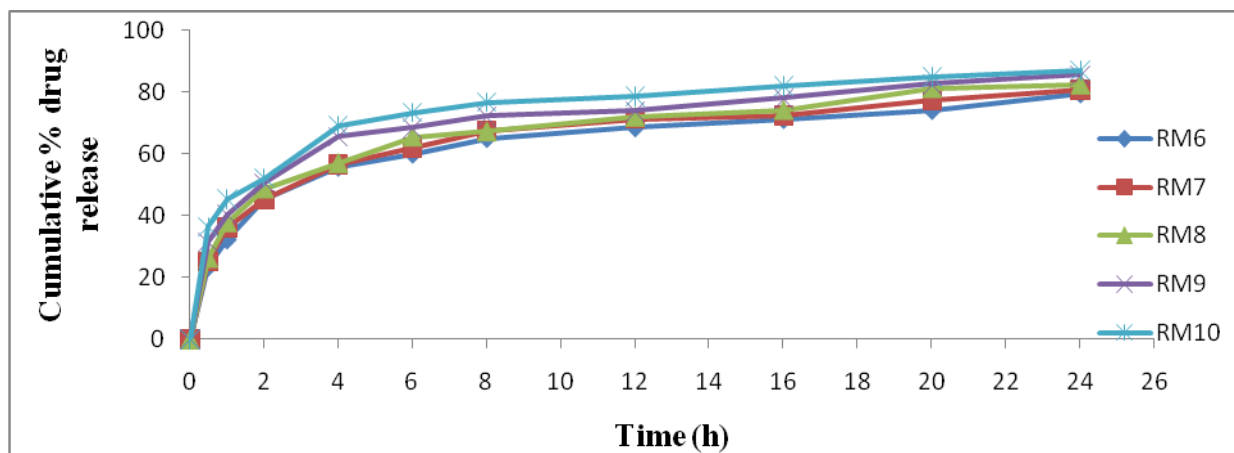**Figure 3: Cumulative % drug release from formulations**

Table 8: Summary of parameters obtained from kinetic analysis of RM6

Zero Order	**Slope(K)**	2.423
	Intercept	31.84
	r^2	0.675
First Order	**Slope(K/2.303)**	-0.023
	K	-0.06909
	Intercept	1.828
	r^2	0.849
Higuchi's model	**Slope(K)**	14.37
	Intercept	16.84
	r^2	0.882
Korsemeyer-Peppas model	**Slope(n)**	0.588
	Intercept(log K)	1.188
	K	24.60
	r^2	0.393

3.5 Morphological analysis

The morphological characteristics of selected metronidazole loaded chitosan nanoparticle formulation (RM6) was examined using SEM. The nanoparticles were seen to be distinct,

Citation: Ruchika et al. Ijsrm.Human, 2016; Vol. 4 (4): 1-17.

13

spherical particles with solid dense structure. The SEM image of metronidazole loaded chitosan nanoparticle (Figure 4) reveals that the nanoparticles size did not correlate well with the size measured by photon particle size analyzer. The differences in particle size results observed of SEM and particle size analyzer might be attributed to swelling property of chitosan on presence of water.
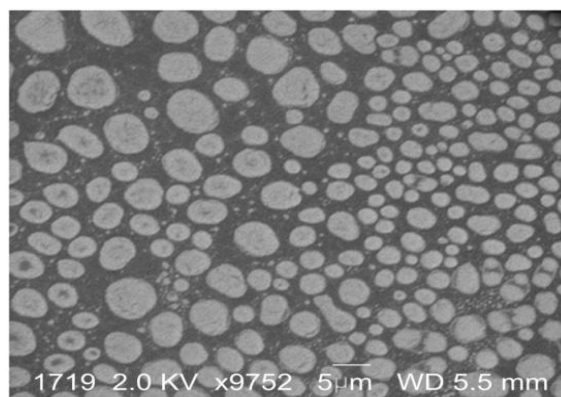
Figure 4: SEM of metronidazole loaded chitosan nanoparticles

3.6 FTIR analysis

IR spectrum of pure metronidazole, chitosan and selected metronidazole loaded chitosan nanoparticle formulation (RM6) are shown in Figure 5, 6, 7. Interestingly, in IR spectrum of the selected metronidazole loaded chitosan nanoparticles formulation (RM6), the peak at 1657 cm^{-1} (attributed to the amide group in chitosan) was absent and a new peak appeared at 1593 cm^{-1}. The peak at 1565 cm^{-1} (ascribed to $-NH_2$ in chitosan) shifted to ~ 1530 cm^{-1} which reflects the cross-linking between tripolyphosphoric group of TPP and $-NH_2$ group of chitosan. The peak displayed at 1230 cm^{-1} corresponds to P=O stretching. Also, shift in the peak observed at 1481 cm^{-1} (due to the $-NO_3$ group in metronidazole) to 1414 cm^{-1} may be attributed to involvement of the group in intermolecular hydrogen bonding.

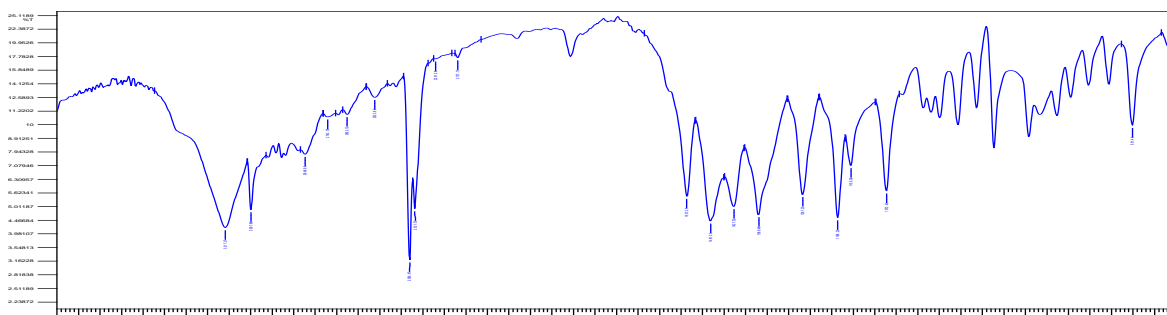*Citation: Ruchika et al. Ijsrm.Human, 2016; Vol. 4 (4): 1-17.*
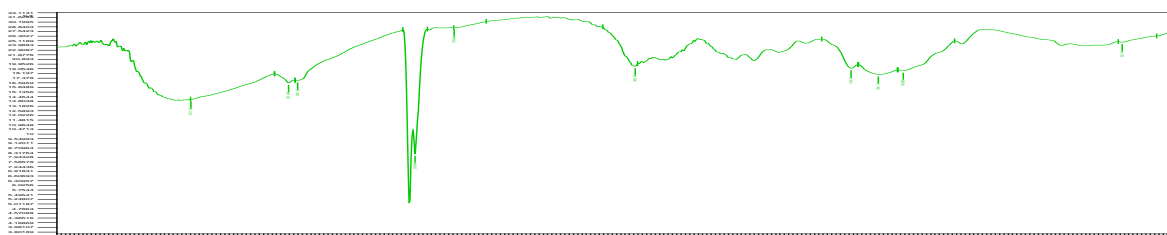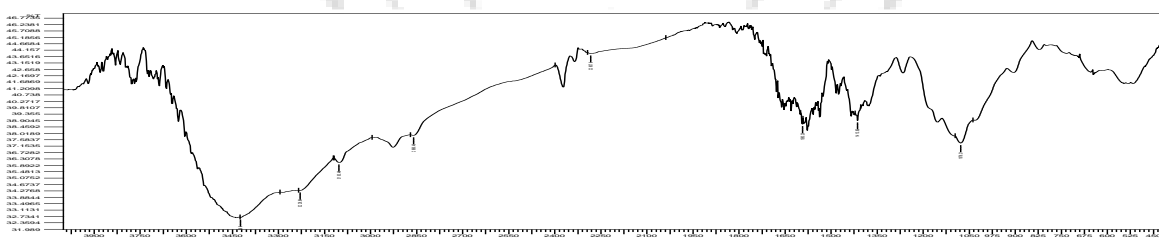
14

Figure 5: FT-IR spectrum of metronidazole

Figure 6: FT-IR spectrum of chitosan

ure 7: FT-IR spectrum of metronidazole loaded nanoparticles

3.7 Differential Scanning Calorimetry analysis

Thermal analysis of pure metronidazole, chitosan and selected metronidazole loaded chitosan nanoparticles formulation (RM6) were carried out using DSC and respective thermograms are shown in Figure 8, 9, 10. The endotherm of metronidazole shifted to the lower temperature in selected metronidazole loaded chitosan nanoparticle formulation (RM6). Decreased crystallinity indicates change in solid state structure of chitosan due to cross-linking. Parallel results were obtained with catechin loaded chitosan nanoparticles.[129] Vikas Kumar, Dinesh, Rakesh and Ashok (2004)[219] reported similar shifts in DSC plots of CS and CS NPs.
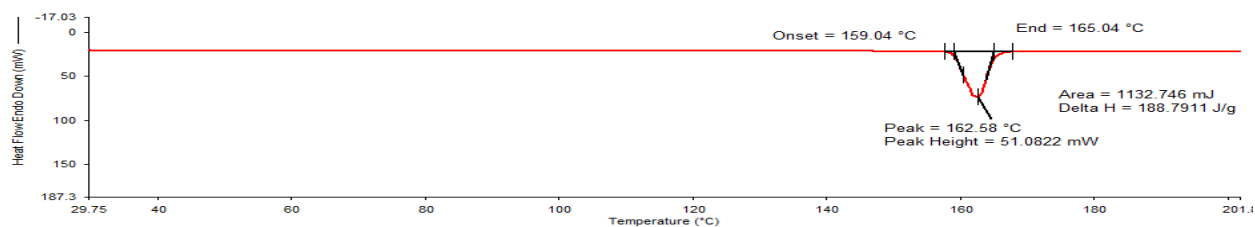
Citation: Ruchika et al. Ijsrm.Human, 2016; Vol. 4 (4): 1-17.

15

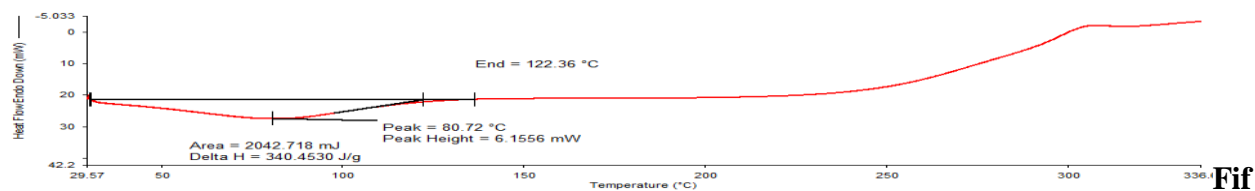**Figure 8: DSC Thermogram of pure metronidazole**
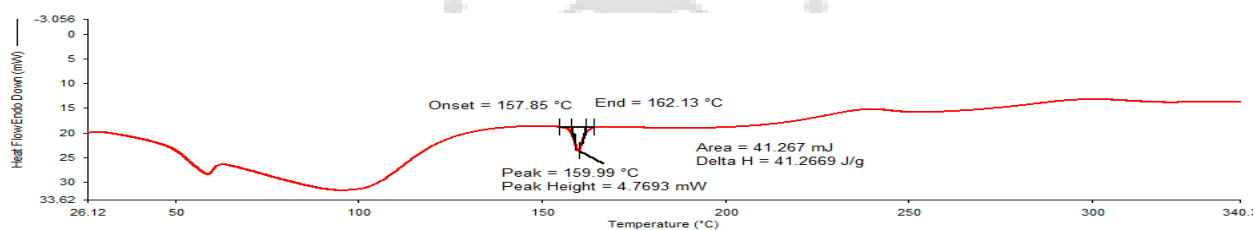

Figure 9: DSC Thermogram of chitosan

Figure 10: DSC Thermogram of metronidazole loaded chitosan nanoparticles

4. CONCLUSION

The metronidazole loaded chitosan nanoparticles were successfully prepared by cross-linking with TPP. The nanoparticles were stable and spherical in shape with a narrow size distribution. Different percentage entrapment efficiency and loading capacity of metronidazole were obtained by varying the mass ratio of metronidazole in different formulations and also the varied percentage of adhered nanoparticles were obtained by changing the mass ratio of chitosan and metronidazole. *In-vitro* release studies showed that the drug is released from the formulation over a period of 24 h in a sustained manner and the release mechanism followed a Non-Fickian type behaviour. The release amount of metronidazole from chitosan nanoparticles suggested that metronidazole loaded chitosan nanoparticles have promising potential effect on colon-specific drug delivery. However, in future *in-vivo* studies should be conducted on metronidazole loaded chitosan nanoparticles so that such formulations could find place in the pharma market.

Citation: Ruchika et al. Ijsrm.Human, 2016; Vol. 4 (4): 1-17.

16

REFERENCES

1. Sailaja AK, Amareshwar P, Chakravarty P. Chitosan nanoparticles as a delivery system. Res J Pharm Bio Chem Sci. 2010; 1(3): 474-484.

2. Panyam J, Labhasetwar V. Biodegradable nanoparticles for drug and gene delivery to cells and tissue. Adv Drug Deliv Rev. 2012; 64: 61-71.

3. Nagpal K, Singh SK, Mishra DN. Chitosan Nanoparticles: A Promising System in Novel Drug Delivery. Chem Pharm Bull. 2010; 58(11): 1423-1430.

4. Tiyaboonchai W. Chitosan Nanoparticles: A Promising system for drug delivery. Naresuan Uni J. 2003; 11(3): 51-66.

5. Bowman K and Leong KW. Chitosan nanoparticles for oral drug and gene delivery. Int J Nanomed. 2006; 1(2): 117-128.

6. Dash M, Chiellini F, Ottenbrite RM, Chiellini E. Chitosan: A versatile semisynthetic polymer in biomedical applications. Prog Polym Sci. 2011; 36: 981-1014.

7. Sonia TA and Sharma CP. Chitosan and its Derivatives for Drug Delivery Perspective. Adv Polym Sci. 2011; 243: 23-54.

8. Bansal V, Sharma PK, Sharma N, Pal OP, Malviya R. Applications of Chitosan and Chitosan Derivatives in Drug Delivery. Adv Bio Res. 2011; 5(1): 28-37.

9. Chourasia MK and Jain SK. Pharmaceutical approaches to colon targeted drug delivery systems. J Pharm Pharm Sci. 2003; 6(1): 33-66.

10. Sharma A, Jain KA. Colon targeted drug delivery using different approaches. Int J Pharm Studies Res. 2010; 1(1): 60-66.

11. Singh N, Khanna RC. Colon targeted drug delivery systems: A potential approach. The Pharma Innovation. 2012; 1(1): 40-47.

12. Tiwari G, Tiwari R, Wal P, Wal A, Rai AK. Primary and novel approaches for colon targeted drug delivery: A review. Int J Drug Deliv. 2010; 2: 1-11.

13. Zhang H, Alsarra IA, Neau SH. An in vitro evaluation of a chitosan-containing multiparticulate system for macromolecule delivery to the colon. Int. J. Pharm. 2002; 239: 197-205.

14. Agnihotri SA, Mallikarjuna NN, Aminabhavi TM. Recent advances on chitosan-based micro and nanoparticles in drug delivery. J Contr Release. 2004; 100: 5-28.

15. Elzatahry AA, Mohy Eldin MS. Preparation and characterization of metronidazole loaded chitosan nanoparticles for drug delivery application. Polym Adv Technol. 2008; 19: 1787–1791.

16. Mishra AK, Yadav R, Mishra A, Verma A, Chattopadhyay P. Development and validation of UV spectrophotometric method for the determination of metronidazole in tablet formulation. Int J Pharm Res Dev. 2012; 2(6): 1-5.

17. Latha S, Selvamani P, Kumar CS, Sharavanan P, Suganya G, Beniwal VS, Rao PR. Formulation development and evaluation of metronidazole magnetic nanosuspension as a magnetic-targeted and polymeric-controlled drug delivery system. J Magnetism Magnetic Materials. 2009; 321: 1580-1585.

18. Patel Gn, Patel RB, Patel HR. Formulation and in-vitro evaluation of microbially triggered colon specific drug delivery using sesbania gum. e-J Sci Tech. 2011; 6(2): 33-45.

19. Krishnaiah YSR, Reddy PRB, Satyanarayana V, Karthikiyan RS. Studies on the development of oral colon targeted drug delivery systems for metronidazole in the treatment of amoebiasis. Int J Pharm. 2002; 236: 43–55.

20. Mehta TJ, Rajput SS, Patel MR, Patel KR, Patel NM, Mothilal M. Formulation development and optimization of metronidazole compression coated tablets. Der Pharmacia Lett. 2011; 3(5): 94-103.

21. Kumar MP, Ishaq BM, Reddy JRK, Kumar RP, Badrinath A, Chetty CM. Formulation and evaluation of colon specific matrix and coated tablet of metronidazole. Int Res J Pharm. 2011; 2(9): 194-199.

Citation: Ruchika et al. Ijsrm.Human, 2016; Vol. 4 (4): 1-17.

17